

See discussions, stats, and author profiles for this publication at: <https://www.researchgate.net/publication/6679861>

Very High Third-Order Nonlinear Optical Activities of Intrazeolite PbS Quantum Dots

ARTICLE *in* JOURNAL OF THE AMERICAN CHEMICAL SOCIETY · DECEMBER 2006

Impact Factor: 12.11 · DOI: 10.1021/ja0661966 · Source: PubMed

CITATIONS

43

READS

26

6 AUTHORS, INCLUDING:



[Hyun Sung Kim](#)

Pukyong National University

879 PUBLICATIONS 15,372 CITATIONS

[SEE PROFILE](#)



[Nak Cheon Jeong](#)

Daegu Gyeongbuk Institute of Science and T...

38 PUBLICATIONS 1,283 CITATIONS

[SEE PROFILE](#)

Very High Third-Order Nonlinear Optical Activities of Intrazeolite PbS Quantum Dots

Hyun Sung Kim,[†] Myoung Hee Lee,[†] Nak Cheon Jeong,[†] Seung Mook Lee,[‡] Bum Ku Rhee,[‡] and Kyung Byung Yoon^{*†}

Center for Microcrystal Assembly, Department of Chemistry, and Program of Integrated Biotechnology, Sogang University, Seoul 121-742, Korea, and Department of Physics, Sogang University, Seoul 121-742, Korea

Received August 25, 2006; E-mail: yoonkb@sogang.ac.kr

Semiconductor quantum dots (QDs) dispersed in glass and polymer matrixes have shown third-order nonlinear optical (3NLO) properties^{1–12} which can be exploited for fabrication of optical switches, waveguides, optical limiters, and many others. However, their sensitivities have not yet reached to the degrees sufficient for practical applications.

Zeolites are excellent hosts for QDs^{13–21} and have many advantages over glass and polymers due to the following. The zeolite-encapsulated QDs are usually smaller than 1.5 nm; their sizes are highly uniform, and they exist very regularly within the crystalline hosts. Despite the above characteristics, the measurements of the 3NLO properties of zeolite-encapsulated QDs have not been made due to the difficulty of preparing zeolite films supported on optically transparent substrates, such as glass and quartz, with reasonably high binding strengths between the films and substrates. For instance, when zeolite-Y films are grown on ordinary glass or fused silica, they readily peel off the substrates during drying, ion exchange with other ions, and calcination to remove organic contaminants. Furthermore, the strong tendency of many QDs to be expelled from the zeolite pores to the external surfaces by moisture²¹ has also hampered the measurements.

We now report that zeolite-Y films grown on the surfaces of indium-tin-oxide-coated (ITO) glass plates remain firmly bonded to the substrates during ion exchange with Pb²⁺ ions, drying, and formation of PbS by treating Pb²⁺ ions with H₂S and that the encapsulated PbS QDs show very high 3NLO activities.

The zeolite-Y films (thickness = 2 μm) supported on ITO glass (denoted as Y_g, average size = ~2 × 2.5 cm²) were prepared according to the procedure described in SI-1. The surface-polished Y_gs (thickness = 1.5 μm) became transparent (SI-2). Several Y_gs loaded with different numbers (*n* = 0, 8, 14, 23, and 33) of PbS in a unit cell were prepared [denoted as (PbS)_{*n*}-Y_g] according to the procedure described in SI-3.

The intrazeolite PbS QDs slowly migrated from the interior to the external surfaces and formed 3–20 nm-sized PbS QDs on the external surfaces upon exposure of (PbS)_{*n*}-Y_g (*n* ≥ 8) to the atmosphere (SI-4). To prevent the above phenomenon, the surfaces of dry (PbS)_{*n*}-Y_g were coated with octadecyl groups using octadecyltrimethoxysilane (ODM) in a glove box charged with dry argon (SI-5). Analyses of Pb²⁺-exchanged Y, moisture-exposed (PbS)_{*n*}-encapsulating Y, and ODM-coated (PbS)_{*n*}-encapsulating Y crystals with transmission electron microscope (TEM) (SI-4), ²⁷Al and ²⁹Si NMR spectra (SI-6), and X-ray diffraction patterns (SI-7) revealed that the formation of PbS results in partial framework rupture, due to simultaneous incorporation of H⁺ during the process of PbS formation.¹⁷ Furthermore, the analyses revealed that ODM coating effectively prevents PbS QDs from leaving the internal

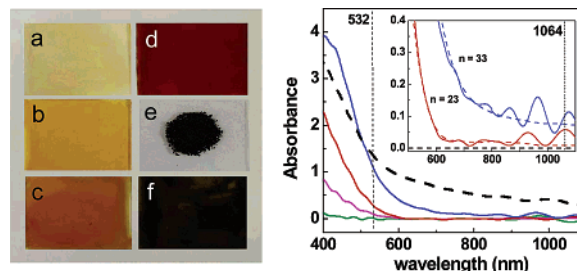


Figure 1. Left: The photographs of ODM-(PbS)_{*n*}-Y_g for 8 (a), 14 (b), 23 (c), and 33 (d), the bulk PbS powder on a Y_g plate (e), and moist (PbS)₃₃-Y_g (f). Right: Absorption spectra of ODM-(PbS)_{*n*}-Y_g for *n* = 8 (green), 14 (pink), 23 (red), and 33 (blue), and moist-(PbS)₃₃-Y_g (black dash). Inset: Enlarged spectra of *n* = 23 and 33 in the 500–1100 nm region. The dashed curves represent the corresponding estimated absorption spectra free from interference patterns.

Table 1. 3NLO Activities of (PbS)_{*n*}-Intercalating Zeolite-Y Films

ODM-(PbS) _{<i>n</i>} -Y _g <i>n</i>	532 nm		1064 nm	
	γ (×10 ⁻¹² cm ² /W)	β (cm/GW)	γ (×10 ⁻¹² cm ² /W)	β (cm/GW)
8				
14	-11	85		
23	-34	290	-32	-72
33	-294 (-6) ^a	5900 (-50) ^a	-130 (-1) ^a	-1440 (46) ^a
33 (moist)		45		

^a Highest literature values (ref 7).

pores, as in other cases (SI-4).²¹ The ODM-coated and moisture-exposed (PbS)_{*n*}-Y_gs are denoted as ODM-(PbS)_{*n*}-Y_g and moist-(PbS)_{*n*}-Y_g, respectively.

The color of ODM-(PbS)_{*n*}-Y_g progressively red-shifted from pale yellow to deep red with increasing *n* (Figure 1, left, a–d). The colors were distinctively different from black, the color of bulk PbS (e). The color of moist-(PbS)₃₃-Y_g was black (f), consistent with the presence of large PbS QDs (3–20 nm) on the external surfaces. The absorption (Figure 1, right) spectra show that the amount of PbS QDs that absorb at 532 nm increases with increasing *n*. The enlarged spectra (inset) further revealed that the samples with *n* = 23 and 33 contain intrazeolite QDs that absorb even at 1064 nm, although very weakly (abs = 0.01 and 0.07, respectively). Moist-(PbS)₃₃-Y_g showed absorption over the entire visible region and even beyond 1100 nm (Figure 1, right, black dashed curve), due to large PbS QDs existing on the external surfaces (see SI-8 for the verification of QDs within zeolite and the nonexistence of excitonic bands in the spectra).

The nonlinear refraction (γ) and absorption (β) coefficients (SI-7) of the films at 532 and 1064 nm, respectively, are shown in Table 1. They were measured using the *z*-scan method (SI-9) using mode-locked picosecond laser pulses (pulse width = 50 ps) at two

[†] Department of Chemistry.

[‡] Department of Physics.

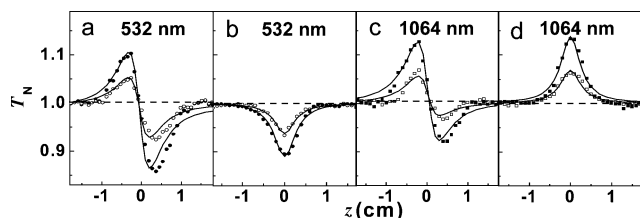


Figure 2. The z -scan data (symbols) and theoretically fitted curves (solid curves) of ODM-(PbS)₃₃-Y_g obtained under the closed (a) and open (b) aperture conditions at 532 nm and under the closed (c) and open (d) aperture conditions at 1064 nm. Input irradiances at the focal point were 0.10 and 0.18 GW/cm² at 532 nm and 0.27 and 0.47 GW/cm² at 1064 nm.

different pulse powers. Figure 2 represents the plots of the normalized transmittance (T_N) versus the propagation path (z) of a focused quasi-Gaussian beam of ODM-(PbS)₃₃-Y_g. The threshold pulse powers that start damaging the zeolite films were 5.23 (at 532 nm) and 2.51 (at 1064 nm) GW/cm², respectively.

The 3NLO activity of ODM-(PbS) _{n} -Y_g at 532 nm increased with increasing n , in correlation with the absorption intensity at the wavelength. The absence of activities from the samples with $n = 0$ and 8 shows that the 3NLO activity does not come from the bare zeolite film, ITO glass substrate, or surface-coated ODM. Similarly, the activity at 1064 nm increased in correlation with the absorption intensity of PbS QDs at the wavelength ($n \geq 23$). The above results unambiguously show that the active species are intrazeolite PbS QDs, and their 3NLO activities occur by resonant processes (the responses that are triggered by absorption of QD). The fact that moist-(PbS)₃₃-Y_g gave very weak 3NLO response shows that, while the intrazeolite PbS QDs are active, the large external PbS QDs are not or weakly active.

The obtained γ and β values of ODM-(PbS)₃₃-Y_g at 532 nm are larger by 47 and 118 times, respectively, in magnitude than the highest values ever measured from PbS QDs (−6 and −50, respectively),⁷ and the values at 1064 nm are larger by 130 and 31 times, respectively, in magnitude than the highest values ever measured from PbS QDs (−1 and 46, respectively) under similar input pulse conditions.⁷ The values at 1064 nm are still larger by 23 and 18 times than the values observed from GaAs dispersed in vycor glass,⁵ which are the highest values ever observed from QDs.

The negative γ values reveal that the PbS QDs show a self-defocusing behavior at both wavelengths. The β values are positive (at 532 nm) and negative (at 1064 nm), indicating that the PbS QDs behave as strong excited-state absorbers and optical bleachers, respectively, at the corresponding wavelengths. Opposite signs of β were observed from larger PbS QDs dispersed in polyvinyl alcohol.⁷ The measured relaxation time of PbS QDs at 532 nm was less than 100 ps (SI-10), which is short enough for them to be applied for optical switching devices.

The 3NLO activities of PbS QDs in other media were also measured by others at various wavelengths with various pulse widths.^{8–12} Since the 3NLO activity varies with varying pulse width and wavelength of the laser beam, comparison of the figures of merit ($\chi^{(3)}/\alpha_0$ and γ/α_0 , where $\chi^{(3)} = 3\text{NLO susceptibility}$ and $\alpha_0 = \text{linear absorption coefficient}$) should be conducted when the data were obtained under similar measurement conditions. The $\chi^{(3)}/\alpha_0$ and γ/α_0 of ODM-(PbS)₃₃-Y_g were $3.4 \times 10^{-12} \text{ esu}\cdot\text{cm}$ and $-4 \times 10^{-14} \text{ cm}^2/\text{W}\cdot\text{cm}$ at 532 nm and $2.3 \times 10^{-11} \text{ esu}\cdot\text{cm}$ and $-2.8 \times 10^{-13} \text{ cm}^2/\text{W}\cdot\text{cm}$ at 1064 nm, respectively. When compared with the γ/α_0 value reliably obtained from 2.3 to 3.5 nm PbS QDs dispersed in silica–titania film ($-5 \times 10^{-15} \text{ cm}^2/\text{W}\cdot\text{cm}$, see SI-11),¹¹ which was measured under similar conditions (60 ps pulse width at 1064 nm), the γ/α_0 value of ODM-(PbS)₃₃-Y_g is more than 56 times higher.

The fact that the 3NLO activities of ODM-(PbS) _{n} -Y_g occur by resonant processes indicates that the activities originate from the laser-induced transient changes in the absorption spectra.¹ The following are proposed to cause the very high 3NLO activities. The sizes of QDs (<1.5 nm) are smaller than those that have been dispersed in other media (>2.5 nm) due to encapsulation in zeolite pores. Second, zeolite pores can accommodate a large number of QDs without transforming them to larger QDs due to the rigidity of the pore systems. Third, the strong electric field within the pores greatly stabilizes the generated excitons, which also provides the opportunity to form even biexcitons, whose formation is favored with decreasing the QD size.²

This work thus reports for the first time that zeolite-encapsulated PbS QDs show very high 3NLO activities. Since there are many different types of QDs and many different types of zeolites with different pore sizes, pore shapes, pore networking, framework compositions, and cations, we expect that the development of 3NLO materials with much higher sensitivities operable at various wavelengths is just a matter of time. Thus, this work provides not only a promising new direction to which the search for highly sensitive 3NLO materials has to be conducted but also a new direction to which zeolite research and applications have to be expanded.

Acknowledgment. We thank the Ministry of Science and Technology and Sogang University for supporting this work through the Creative Research Initiatives and the Internal Research Fund programs, respectively.

Supporting Information Available: Experimental procedures, SEM and TEM images, solid-state NMR spectra, and X-ray diffraction pattern. This material is available free of charge via the Internet at <http://pubs.acs.org>.

References

- (1) Wang, Y. *Acc. Chem. Res.* **1991**, *24*, 133–139.
- (2) Hu, Y. Z.; Lindberg, M.; Koch, S. W. *Phys. Rev. B* **1990**, *42*, 1713–1723.
- (3) Guerreiro, P. T.; Ten, S.; Borrelli, N. F.; Butty, J.; Jabbour, G. E.; Peyghambarian, N. *Appl. Phys. Lett.* **1997**, *71*, 1595–1597.
- (4) Wang, Y.; Wang, M.; Yao, X.; Kong, F.; Zhang, L. *J. Cryst. Growth* **2004**, *268*, 575–579.
- (5) (a) Justus, B. L.; Tonucci, R. J.; Berry, A. D. *Appl. Phys. Lett.* **1992**, *61*, 3151–3153. (b) Dvorak, M. D.; Justus, B. L.; Berry, A. D. *Opt. Commun.* **1995**, *116*, 149–152.
- (6) Zhu, Y.; Elim, H. I.; Foo, Y.-L.; Yu, T.; Liu, Y.; Ji, W.; Lee, J.-Y.; Shen, Z.; Wee, A. T.-S.; Thong, J. T.-L.; Sow, C.-H. *Adv. Mater.* **2006**, *18*, 587–592.
- (7) Yu, B.; Yin, G.; Zhu, C.; Gan, F. *Opt. Mater.* **1998**, *11*, 17–21.
- (8) Lu, S.-W.; Sohling, U.; Mennig, M.; Schmidt, H. *Nanotechnology* **2002**, *13*, 669–673.
- (9) Liu, B.; Li, H.; Chew, C. H.; Que, W.; Lam, Y. L.; Kam, C. H.; Gan, L. M.; Xu, G. Q. *Mater. Lett.* **2001**, *51*, 461–469.
- (10) Huang, W.; Shi, J. *J. Mater. Res.* **2000**, *15*, 2343–2346.
- (11) Martucci, A.; Fick, J.; Schell, J.; Battaglin, G.; Guglielmi, M. *J. Appl. Phys.* **1999**, *86*, 79–87.
- (12) Ai, X.; Guo, L.; Zou, Y.; Li, Q.; Zhu, H. *Mater. Lett.* **1999**, *38*, 131–135.
- (13) Wang, Y.; Herron, N. *J. Phys. Chem.* **1987**, *91*, 257–260.
- (14) Moller, K.; Eddy, M. M.; Stucky, G. D.; Herron, N.; Bein, T. *J. Am. Chem. Soc.* **1989**, *111*, 2564–2571.
- (15) Stucky, G. D.; Mac Dougall, J. E. *Science* **1990**, *247*, 669–678.
- (16) Liu, X.; Thomas, J. K. *Langmuir* **1989**, *5*, 58–66.
- (17) (a) Leiggener, C.; Calzaferri, G. *Chem.-Eur. J.* **2005**, *11*, 7191–7198. (b) Leiggener, C.; Calzaferri, G. *Chem. Phys. Chem.* **2004**, *5*, 1593–1596.
- (18) Terasaki, O.; Yamazaki, K.; Thomas, J. M.; Ohsuna, T.; Watanabe, D.; Sanders, J. V.; Barry, J. C. *Nature* **1987**, *330*, 58–60.
- (19) Armand, P.; Saboungi, M.-L.; Price, D.-L.; Iton, L.; Cramer, C.; Grimsditch, M. *Phys. Rev. Lett.* **1997**, *79*, 2061–2064.
- (20) Ozin, G. A.; Steele, M. R.; Holmes, A. J. *Chem. Mater.* **1994**, *6*, 999–1010.
- (21) Jeong, N. C.; Kim, H. S.; Yoon, K. B. *Langmuir* **2005**, *21*, 6038–6047.

JA0661966

Very High Third-Order Nonlinear Optical Activities of Intrazeolite PbS Quantum Dots

Supporting Information

SI-1. Preparation of Y_g s

The Y_g s ($2 \times 2.5 \text{ cm}^2$) were prepared according to the procedure described in our previous report (ref 21 in the text, Jeong, N. C.; Kim, H. S.; Yoon, K. B. *Langmuir* **2005**, 21, 6038.) using ITO glass plates instead of ordinary glass plates. The average thickness of the pristine zeolite-Y films was $2.0 \mu\text{m}$. After polishing them with a piece of fine cloth and alumina powders ($0.3 \mu\text{m}$), the pristine, opaque zeolite Y films became transparent and the average thickness decreased to $1.5 \mu\text{m}$.

SI-2. SEM and photographic images of Zeolite-Y films

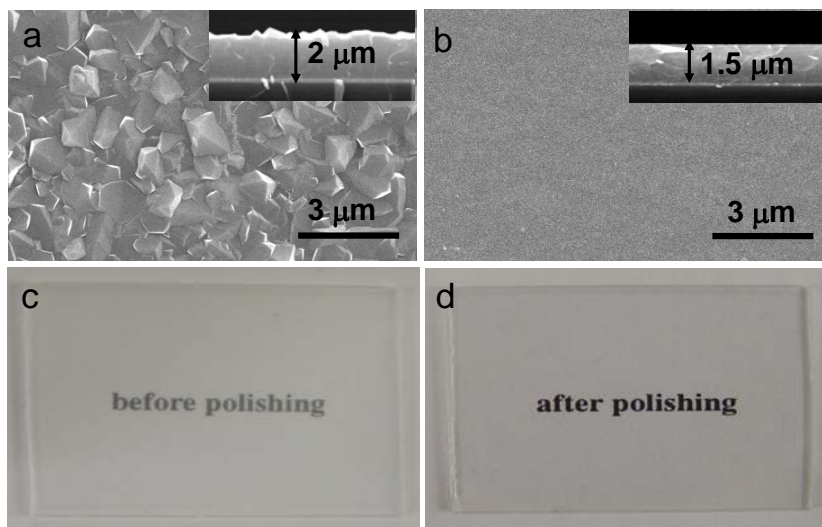


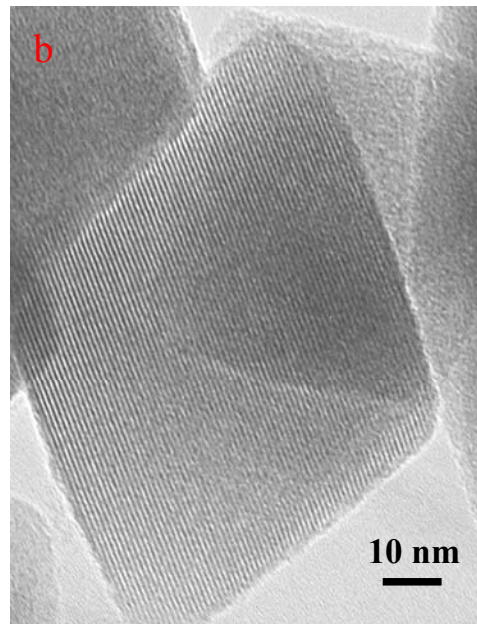
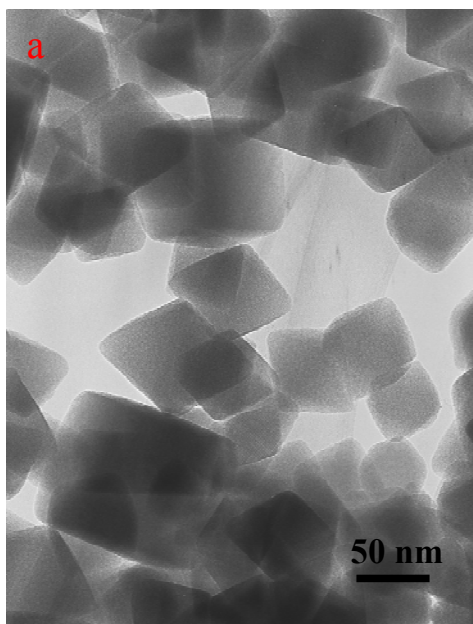
Figure. SEM images (top views) of zeolite-Y films grown on ITO glass plates (Y_g s) before (a) and after (b) polishing and the photographs of an Y_g before (c) and after (d) polishing. The SEM images in the insets of (a) and (b) show the corresponding cross sections.

SI-3. Preparation of (PbS)_n-intercalating Y_gs [(PbS)_n-Y_g]

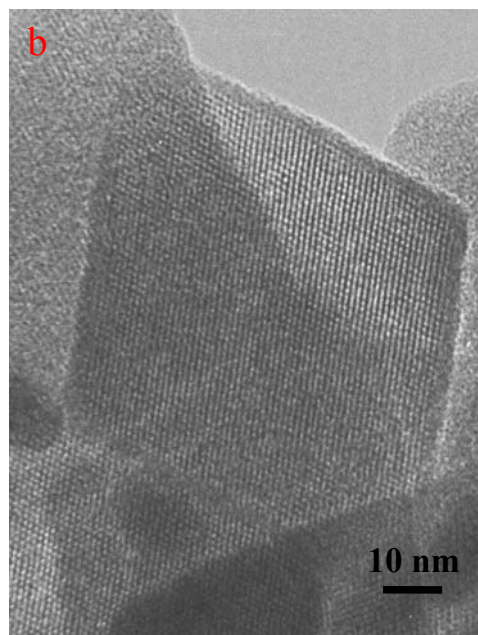
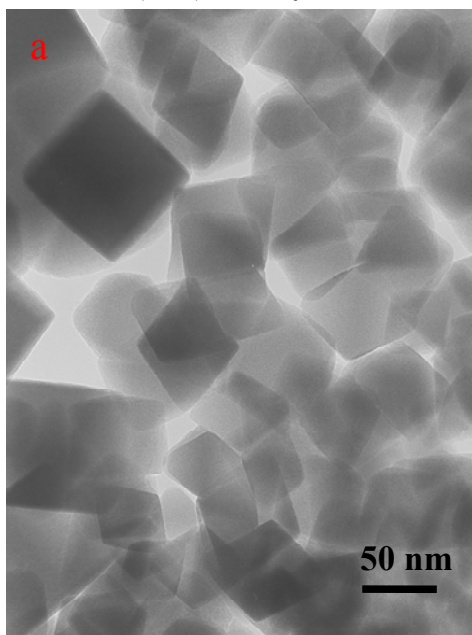
An Y_g (zeolite-Y film grown on ITO glass) plate was immersed into each 25-mL aliquot of Pb(NO₃)₂ solutions of different concentrations (x mM, x = 0.1, 0.4, 1, and 10) for 30 min at room temperature. The removed Pb²⁺-exchanged Y_g [(Pb)-Y_g] was washed with copious amounts of distilled deionized water, and dried by blowing nitrogen onto the film. The amount of Pb²⁺ ions per unit cell in each (Pb)-Y_g was 8, 14, 23, and 33, respectively. The (Pb)-Y_gs were then introduced into a Schlenk tube and then dried at 200 °C for 12 h under vacuum (< 10⁻⁵ Torr). Dry H₂S gas (Rigas, 99.5%) was introduced into the Schlenk tube containing dry (Pb)-Y_g plates at room temperature. After allowing them to react with dry H₂S for 1 h, excess H₂S gas was removed by evacuation of the Schlenk tube for 10 min at room temperature. The compositions were analyzed by both energy dispersive X-ray spectroscopy (EDX) and chemical elemental analyses.

SI-4. TEM images of bare zeolite-Y crystals (A), ODM-(PbS)₃₃-Y crystals (B), and moist-(PbS)₃₃-Y crystals (C) at different magnifications (as indicated).

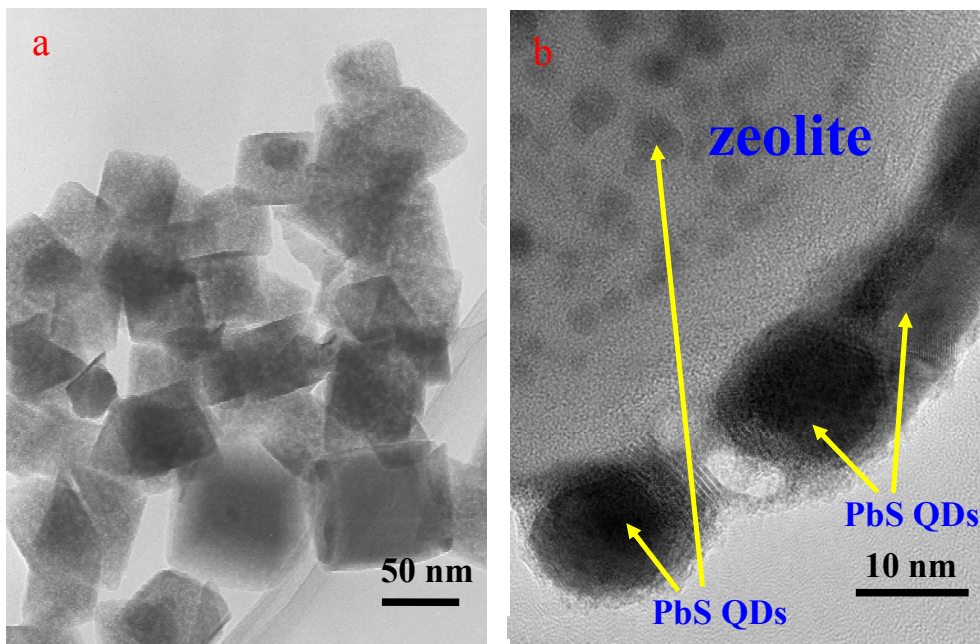
A. Bare zeolite-Y crystals



B. ODM-(PbS)₃₃-Y crystals



C. moist-(PbS)₃₃-Y crystals



For the ease of TEM analyses, we used zeolite-Y crystals [bare zeolite Y crystals, ODM-coated (PbS)₃₃-containing zeolite-Y, and moisture-adsorbed (PbS)₃₃-containing zeolite-Y crystals] instead of bare Y_g, ODM-(PbS)₃₃-Y, and moist-(PbS)₃₃-Y. The zeolite crystals were those that were obtained from the gel which was used for the growth of Y_g. (They were from the same batch.) Therefore, the Si/Al ratios of the above zeolite-Y crystals and Y_g (zeolite-Y films supported on glass) were nearly the same. Zeolite-Y crystals: Si/Al = 1.86, zeolite-Y films: Si/Al ratio = 1.81.

A. TEM images showing the high crystallinity of bare zeolite-Y crystals.

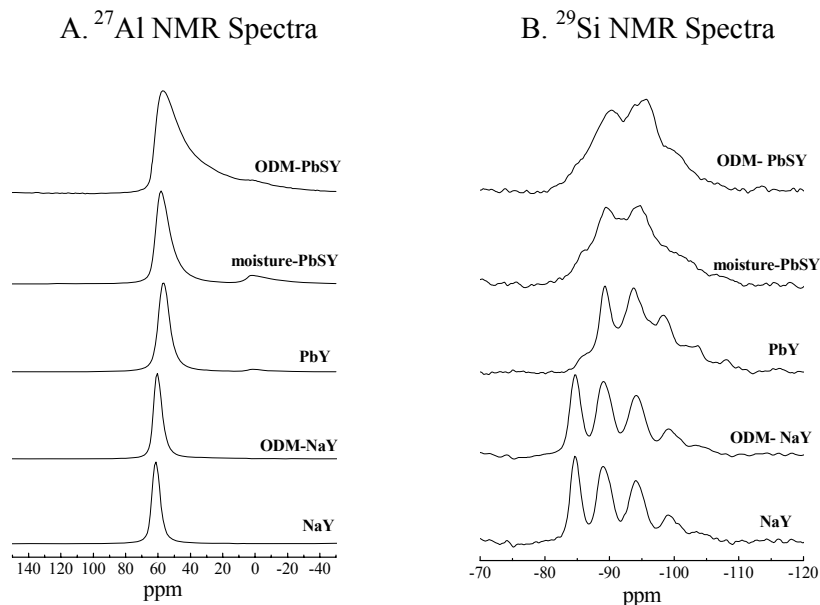
B. TEM images showing that the crystallinity of most of the zeolite-Y crystals were preserved even after production of PbS QDs within the pores, despite the fact that protons (H⁺) were simultaneously generated within the pores, and after coating the surface with ODM. *In this case, although there are PbS QDs within the zeolite crystals, they are not detectable in the above images, indicating that their sizes are smaller than 1.5 nm.*

C. TEM images showing the clear evidence that large PbS QDs (3-20 nm) appear on the surfaces of zeolite-Y upon adsorption of moisture into (PbS)₃₃-Y. Note that the images in B are clearly different from those in C.

SI-5. Surface silylation.

Dry (PbS)_n-Y_{gs} were transferred into a dry box charged with high purity argon and then placed on a Teflon support. The support was immersed into a hexane solution of ODM consisting of 10 mL of ODM and 90 mL of hexane contained in a glass chamber. The chamber with a lid on was placed for 1 h on a hot plate whose temperature was maintained at 60 °C. After cooling the mixture to ambient temperature, the ODM-coated samples were washed with copious amounts of dry *n*-hexane.

SI-6. ²⁷Al NMR and ²⁹Si NMR spectra of bare zeolite Y crystals, (Pb)₃₃-exchanged zeolite-Y, ODM-coated (PbS)₃₃-containing zeolite-Y, and moisture-adsorbed (PbS)₃₃-containing zeolite-Y crystals



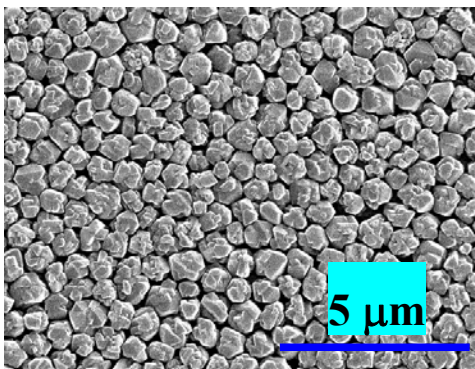
A. The ²⁷Al NMR spectra of bare NaY and ODM-coated NaY are the same, indicating that the ODM-coating does not affect the crystallinity of the zeolite. However, (Pb)₃₃Y shows slight line broadening of the resonance at 57 ppm, due to tetrahedrally coordinated Al atoms, accompanying the simultaneous appearance of a resonance at 0 ppm, due to octahedrally coordinated Al ions, indicating partial framework rupture. Moisture-adsorbed (PbS)₃₃-containing zeolite-Y crystals show that the resonance at 57 ppm is broadened a bit more and

the intensity of the 0-ppm peak increased a bit more, indicating that the partial framework rupture progressed a bit more during the moisture-induced formation of PbS crystals on the surface (see SI-4). However, this shows that the most part of the structure is preserved during the above process. The line broadening of 60-ppm resonance peak underwent even further upon coating the surfaces of dry (PbS)₃₃-containing zeolite-Y crystals with ODM. Since the TEM images of the zeolite crystals (SI-5) showed that the overall crystallinity of the crystals were preserved, the above ²⁷Al NMR spectrum indicates that partial rupture of the internal frameworks underwent during ODM coating.

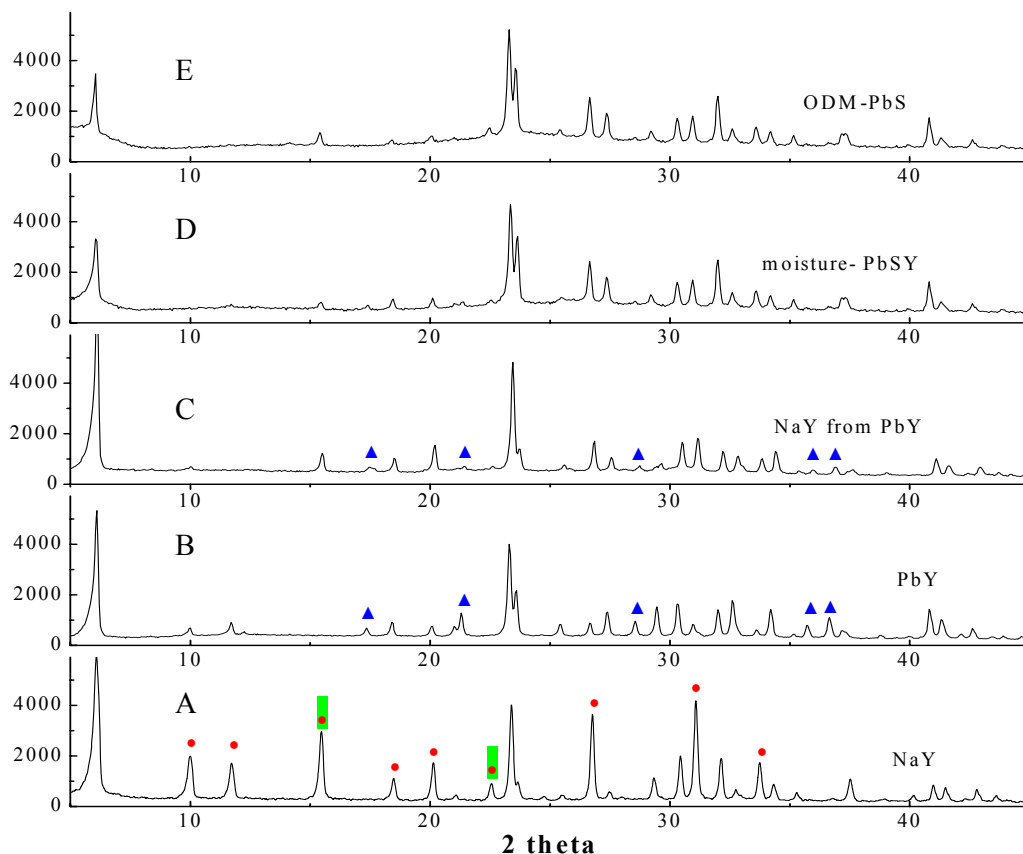
B. The ²⁹Si NMR spectra of bare NaY and ODM-coated NaY are the same, indicating that the ODM-coating does not affect the crystallinity of the zeolite. However, in the case of (Pb)₃₃Y, the intensity of the Q₄ peak decreased accompanying the broadening of other peaks. In the cases of moisture-adsorbed (PbS)₃₃-containing zeolite-Y and ODM-coated (PbS)₃₃-containing zeolite-Y crystals, the degree of line broadening increased even further. Coupled with the fact that the TEM images of the above zeolite crystals (SI-5) showed that their overall crystallinity was preserved, the above NMR spectra indicate that the internal frameworks underwent partial rupture during PbS QD generation.

SI-7. X-ray diffraction patterns of bare zeolite-Y crystals, (Pb)₃₃-exchanged zeolite-Y, ODM-coated (PbS)₃₃-containing zeolite-Y, and moisture-adsorbed (PbS)₃₃-containing zeolite-Y crystals

To check the crystallinity of zeolite Y during the preparation of PbS QDs within the pores, we also prepared zeolite-Y crystals from the same synthesis gel which was used for the synthesis of zeolite Y films on ITO glass. The composition of the gel was 14Na₂O:Al₂O₃:10SiO₂:720H₂O. The crystallization was carried out at 100 °C for 15 h. The average particle size of the crystals was 0.8 μm.



The X-ray powder diffraction patterns were obtained from Rigaku diffractometer (D/MAX-1C) with the monochromatic beam of Cu K α .



X-ray powder diffraction pattern of bare Na⁺-exchanged zeolite-Y (NaY) crystals (panel A) confirmed their structure (zeolite-Y). The diffraction pattern of (Pb)₃₃-exchanged zeolite-Y (panel B) was different from that of NaY. For instance, the peaks in NaY (panel A) marked with a red dot in a green rectangle (■) disappeared and the peaks marked with a red dot (•) significantly decreased while the peaks marked with a blue triangle (▲) newly appeared (panel B). Since the newly appeared small peaks did not disappear even after re-exchange of Pb²⁺ ions with Na⁺ ions (panel C), we conclude that the small peaks appeared due to partial framework rupture during ion exchange of Na⁺ ions with Pb²⁺ ions and ruptured frameworks do not restore back to the original structure even after re-exchange of Pb²⁺ ions with Na⁺ ions. The intensities of the diffraction patterns of moisture-adsorbed (PbS)₃₃-containing zeolite-Y crystals (panel D) and ODM-coated (PbS)₃₃-containing zeolite-Y (panel E) decreased a bit indicating that the crystals underwent minor internal framework rupture during generation of PbS.

SI-8. Verification of the existence of PbS QDs within zeolite-Y.

For the above we obtained the compositions of $(\text{PbS})_n\text{-Y}_g$ samples. The results are summarized in the following table.

Table. Compositions of $(\text{PbS})_n\text{-Y}_g$.

zeolite film	composition
ODM- $[(\text{PbS})_0]\text{-Y}_f$	$\text{Na}_{70.2}\text{Al}_{70.3}\text{Si}_{121.7}\text{O}_{384}$
ODM- $[(\text{PbS})_8]\text{-Y}_f$	Pb_{7.9}S_{7.2} $\text{H}_{14.4}\text{Na}_{54.5}\text{Al}_{70.3}\text{Si}_{121.7}\text{O}_{384}$
ODM- $[(\text{PbS})_{14}]\text{-Y}_f$	Pb_{14.4}S_{14.1} $\text{H}_{28.2}\text{Na}_{41.5}\text{Al}_{70.3}\text{Si}_{121.7}\text{O}_{384}$
ODM- $[(\text{PbS})_{23}]\text{-Y}_f$	Pb_{22.9}S_{22.3} $\text{H}_{44.6}\text{Na}_{24.5}\text{Al}_{70.3}\text{Si}_{121.7}\text{O}_{384}$
ODM- $[(\text{PbS})_{33}]\text{-Y}_f$	Pb_{33.4}S_{33.0} $\text{H}_{66.0}\text{Na}_{3.5}\text{Al}_{70.3}\text{Si}_{121.7}\text{O}_{384}$
moist- $[(\text{PbS})_{33}]\text{-Y}_f$	Pb_{33.4}S_{33.0} $\text{H}_{66.0}\text{Na}_{3.5}\text{Al}_{70.3}\text{Si}_{121.7}\text{O}_{384}\cdot x\text{H}_2\text{O}$

The above compositions were obtained by both energy dispersive X-ray spectroscopy (EDX) analyses and chemical elemental analyses. (The chemical analyses were conducted with the zeolite films that were scraped from the glass substrates.) Both results coincided within the experimental errors.

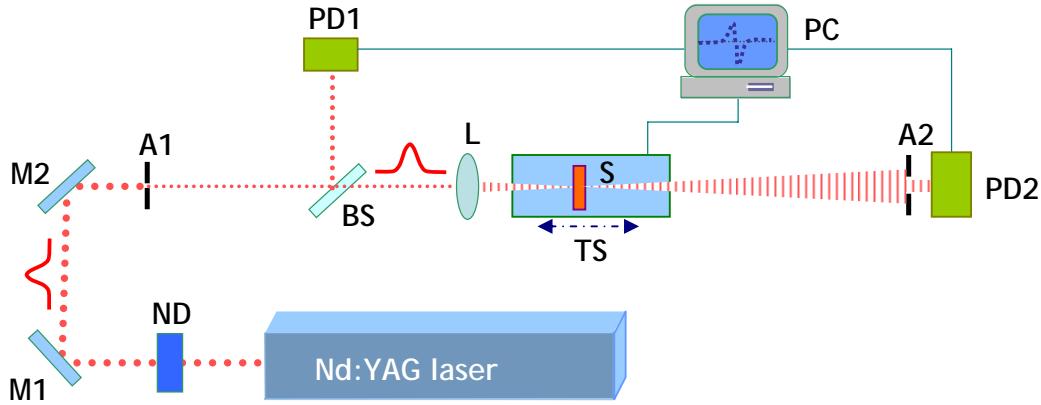
The above elemental analyses clearly showed the 1:1 ratio of both elements (Pb and S) in each zeolite. From the fact that PbS QDs do not exist on the external surface (see SI-4), we conclude that PbS QDs indeed exist within the zeolite frameworks. The existence of PbS QDs within zeolite-Y was also verified by ref 13 in the main text.

The spectra of $(\text{PbS})_n\text{-Y}_g$ (Figure 1, right) did not show the exciton absorption bands. We propose the following two reasons are responsible for the above phenomenon.

- 1) The sizes of QDs are not uniform. We believe that the sizes of PbS QDs vary from subnanometer to ~1.5 nm depending on the number of PbS unit in each QD. Thus, the juxtaposition of many exciton bands at different wavelengths will produce the absorption spectra having no specific envelopes.
- 2) In the case of PbS QDs surrounded by anionic centers such as CO_2^- or SO_3^- the excitonic bands have not been observed despite the fact that the sizes of the PbS QDs were fairly uniform (ref 12 in the main text). Since the zeolite-Y framework is also negatively charged, such an electric field effect may appear in their spectra.

SI-9. Measurements of γ and β values by the Z-scan method.

The γ and β values of the samples were obtained by z-scan technique at 532 and 1064 nm, respectively, using a mode-locked Nd:YAG laser of 50-ps pulse duration with the repetition rate of 10 Hz. The layout of z-scan method used in this work is as follows.



The layout of z-scan method used in this work.

ND: a neutral-density filter for the attenuation of beam power

M1, M2: highly reflecting mirrors for 532 and 1064 nm

A1: (an iris diaphragm) an aperture

A2: (an iris diaphragm) an aperture used only for the closed-aperture Z-scan measurement

BS: a beam splitter

L: a focusing lens with the focal length of 20 cm

S: a sample

TS: a motorized linear translational stage controlled by a PC

PD1: a photodiode for data acquisition of the triggered pulses

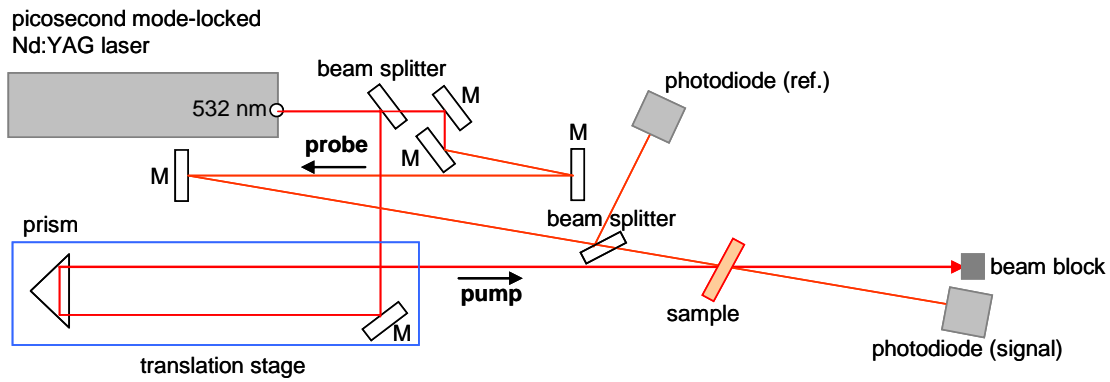
PD2: a photodiode for data acquisition of the signal pulses

The laser beam was split into two parts (~40% and ~60%) using a beam splitter. A part (~40%) of the beam was used to compensate the intensity fluctuation of individual laser pulses. The other part (~60%) was focused using a convex lens (focal length = 20 cm) and directed to the sample. The sample was placed on a stepping-motor-driven translational stage which can traverse along the on-axis of the focused beam in a unit interval of 1 mm. The intensity of the transmitted beam was measured using a Si photodiode (PIN-10D, UDT sensors). In the case of open-aperture z-scan, the whole energy of the transmitted beam was measured. In the case of

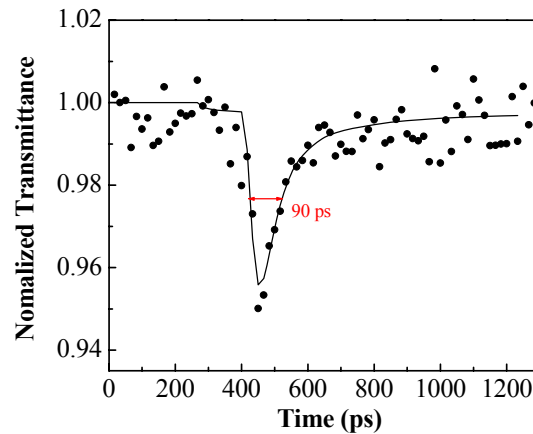
on-axis (closed-aperture) z-scan measurement, an iris was placed in front of the detector. To satisfy the criteria for the on-axis transmittance, the diameter of the iris aperture was made to be 2 mm so that only 1 % of the transmitted beam was collected by the detector. The input irradiance at the focal point (I_0) was 0.10 and 0.18 GW/cm² at 532 nm and 0.27 and 0.47 GW/cm² at 1064 nm.

SI-10.

The relaxation time was measured using the pump-probe set up shown below.



. The typical result is shown below.



SI-11. The estimated γ/α_o of reference 11.

The γ values of silica-titania sol-gel films (thickness 1 μm) doped with various amounts of PbS quantum dots were measured by Martucci et al. (ref 11) using ns and ps laser pulses. Among them the largest γ value was obtained from 25%-loaded sample. The γ value obtained from 25%-loaded sample under the condition that is similar to our case (using picosecond laser pulses with the pulse width of 60 ps and 10 Hz repetition rate) at 1064 nm was $-2 \times 10^{-12} \text{ cm}^2/\text{W}$. Since the authors did not report the absorbance at 1064 nm, we estimated the absorbance from Figure 3 shown below. The estimated absorbance (α_o) of the 25% sample was 0.04. Accordingly, the estimated γ/α_o was $-5 \times 10^{-15} \text{ cm}^2/\text{W}\cdot\text{cm}$

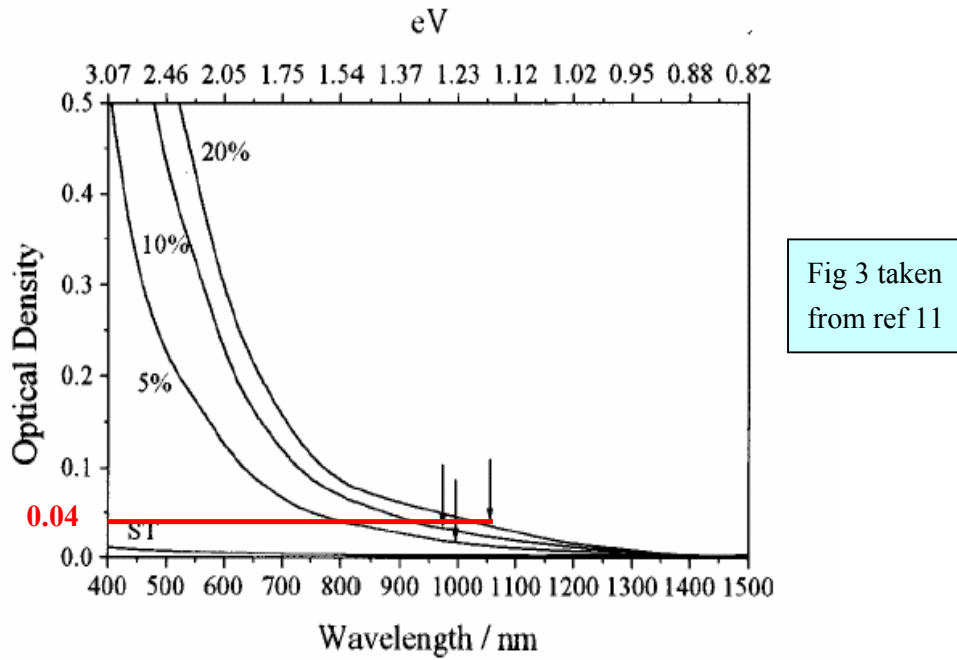


Fig 3 taken
from ref 11

FIG. 3. Absorption spectra of $\text{SiO}_2\text{-TiO}_2$ film doped with 5, 10, and 25 mol % of PbS. The spectrum of an undoped film (ST) is also reported as reference. The arrows indicate the expected position of the first excitonic peak for particles with the mean diameter reported in Table II and estimated by XRD measurements.

Interestingly, however, the % in the caption and the spectra are different. Thus while it is 20% in the figure, it is 25% in the caption. Therefore, the actual absorbance of 25% sample should be higher. If this is the case, the γ/α_o should be smaller than $-5 \times 10^{-15} \text{ cm}^2/\text{W}\cdot\text{cm}$. Note that the γ/α_o from ODM-(PbS)₃₃-Y_g in our result ($-2.8 \times 10^{-13} \text{ cm}^2/\text{W}\cdot\text{cm}$ at 1064 nm.) is larger by 56 times than the value observed from silica-titania sol-gel film doped with 25% PbS QDs.